Case Studies in Construction Materials 15 (2021) e00623

Contents lists available at ScienceDirect

Case Studies in Construction Materials

journal homepage: www.elsevier.com/locate/cscm

Case study

Analysis of vibrations recorded inside the cemetery area of Incisa, central Italy

Riccardo Maria Azzara [a], Stefano Galassi [b,*], Sara Garuglieri [b], Michele Paradiso [b], Marco Tanganelli [b]

[a] Istituto Nazionale di Geofisica e Vulcanologia (INGV), Osservatorio Sismologico di Arezzo, Italy
[b] Università degli Studi di Firenze, Dipartimento di Architettura (DiDA), Italy

ARTICLE INFO

Keywords:
Ambient vibrations
Seismometric measurement
Soil amplification
Transient vibration

ABSTRACT

Seismic stations are usually used to record seismic event and, therefore, they are recommended to be installed far from railways and traffic roads in order to avoid the superposition of ambient noise signals to those provoked by an earthquake. In this paper, instead, seismic stations, placed intentionally in areas near railway and traffic roads, are used to characterize the subsoil spectral properties and to assess the effect of vibrations due to trains and vehicles. A cemetery in the green countryside near Florence is chosen as a reference case study to deal with this topic. Most of the buildings in the cemetery area are affected by an extensive crack pattern. In January 2020 five seismic stations were installed in order to evaluate if the trains running in the tunnels of the regional and high-speed railway lines located below and in the vicinity of the cemetery and the vehicles traveling on the nearby A1 highway and regional road can produce vibrations in the ground that justify the observed damage pattern.

Collected data are analyzed using the Nakamura technique in order to estimate the dynamic properties of the ground and compared to the limits provided by the current regulations. Furthermore, the trend of the Root Mean Square average over the entire recording period is computed as well.

From the obtained results, it is possible to highlight that the average daily oscillation level increases from early morning until 7 p.m. and then it decreases, and also that the highest amplitudes of transients are concentrated in the late evening and during the night, when the background noise is lower.

Furthermore, the computed values of the maximum and average amplitudes are lower than those that can cause damage to buildings as defined by the guidelines, the eigenfrequency of the ground falls in a range far from that ascribable to the cemetery buildings, so that the resonance effects can be excluded. In order to confirm these results, the amplitude of ground shaking due to recorded transients is compared to that produced by two earthquakes (a 3.4 Mw local earthquake at more than 100 km and a Mw 6.6 teleseism from Turkey) which occurred during the monitoring period. One can conclude that it seems unlikely that the shaking produced by nearby vehicles and trains could be responsible for the observed damage.

* Corresponding author.
E-mail addresses: riccardo.azzara@ingv.it (R.M. Azzara), stefano.galassi@unifi.it (S. Galassi), sara.garuglieri@unifi.it (S. Garuglieri), michele.paradiso@unifi.it (M. Paradiso), marco.tanganelli@unifi.it (M. Tanganelli).

https://doi.org/10.1016/j.cscm.2021.e00623
Received 22 March 2021; Received in revised form 30 June 2021; Accepted 14 July 2021
Available online 15 July 2021

1. Introduction

In a classical seismological approach, such as seismic monitoring, train and traffic vibrations are generally considered as noise signals reducing the level of detection of a seismic station; so it is recommended to avoid the installation of seismic stations near railways or trafficked roads. On the other hand, the vibrations induced by railways or vehicular traffic can be an efficient source to geophysically characterize the subsurface and some studies have been published about those subjects [1,2]. From an engineering point of view there is an open debate about the possibility that the vibrations produced by trains and vehicles may be sometimes considered as potential sources of damage (also if moderate or cosmetic) for building structures, especially when they are in close proximity to heavily trafficked railway lines or roads and in particular if they are cultural heritage structures In particular, the spread of high-speed railway lines and the development of tram systems within cities, as solutions to traffic congestion and pollution, has promoted the publication of numerous studies dealing with the subject [3–11].

The study of vibrations (natural or artificial) can be found in a large number of publications ranging from the analysis of the spectral characteristics of the sources to theoretical models describing the propagation in the ground. Also, there are experimental studies aimed at evaluating the effects of vibrations on the ground or on the buildings connected to it (see for example [12–15]). Vibrations can be produced by external sources (vehicular or railway traffic, anthropic activities that produce oscillations on the ground, operation of machines or engines, explosions of mines) that act at the base of the buildings by propagating inside or through forces (movement of people and machines) operating inside. For all these reasons, the identification of physical characteristics of the vibrations complies with specific standards that define the range of values in amplitude and frequency that can produce damaging or disturbing effects to buildings or people. The most recent national policy regarding the measurement of vibrations, devoted to assessing their effects on buildings, is the standard provided by UNI 9916 [16] in 2004, subsequently revised in 2014 and 2017. These standards, which are framed within the regulations in force in Europe, recall the same principles found in the English [17], German [18] and Swiss [19] regulations.

Below we report the analysis of the signals recorded in a cemetery area located very near to railways lines and highly trafficked roads, in order to estimate if the induced vibration on the structures could be responsible for their damage. The analyses were performed both in time and frequency domain with the intent of:

- defining the characteristics of the soil in order to highlight the presence of possible local amplification effects;
- assessing amplitudes and frequencies of the effect of vibrations produced by the railway and vehicular traffic, according to the requirements of the standards, in order to evaluate if they could be considered responsible to for the observed damage pattern;
- analyzing the transient vibrations and the values of the maximum and average amplitudes, as already observed, to determine if these values remain at considerably lower levels than those which, according to the regulations, can cause damage to building structures;
- analyzing the seismograms, considering the recordings of earthquakes that occurred during the installation period of the acquisition system, in order to confirm that the signals produced by daily human activity are indeed of low entity.

2. Subsoil characterization of the investigated area

2.1. Description of the area and of the monitoring system

The cemetery in Incisa, situated in the area known as “I ciliegi” between the towns of Figline and Incisa Valdarno, about 40 km south of Florence, was subjected to seismic monitoring between 20th and 27th January 2020. Five SARA Electronic Instrument devices were installed at the ground level, inside small isolated chapels or in free-field (CIM1), constituted by a 24 bit A/D converter (SL06) coupled to a seismometric sensor with an eigenfrequency of 2 Hz (SS20) or 4.5 Hz (SS45). Table 1 shows the measurement points, indicating the codes of the devices used for each one of them and the length of the monitoring period. Fig. 1b shows the position of the devices.

The signals were recorded at a sample rate of 200 sps; the triaxial seismometers were oriented with the axis Y (component HHN) along the direction indicated in Fig. 1b. Before the analysis, the recorded data had been corrected by the instrument transfer function, in order to enlarge the analysis spectral band.

The stations were synchronized by a GPS (Global Positioning System). The minimal window of contemporaneity of the records of all the seismic stations covers the interval from January, 20th 2020 at 12 o’clock (local time) to January, 23rd 2020 at 7 o’clock (local time), due to the fact that the battery at seismic station CIM3 had drained before the other ones.

Table 1
Devices used in the measurement points.

Code	SS20/45	SL06	Operating period
CIM1	2252	2249	2020-01-20 11:00 (LT) - 2020-01-27 11:00 (LT)
CIM2	2045	1549	2020-01-20 11:00 (LT) - 2020-01-26 15:00 (LT)
CIM3	2251	2248	2020-01-20 11:00 (LT) - 2020-01-23 07:00 (LT)
CIM4	2253	2250	2020-01-20 11:00 (LT) - 2020-01-24 09:00 (LT)
CIM5	2542	2541	2020-01-20 11:00 (LT) - 2020-01-26 18:00 (LT)

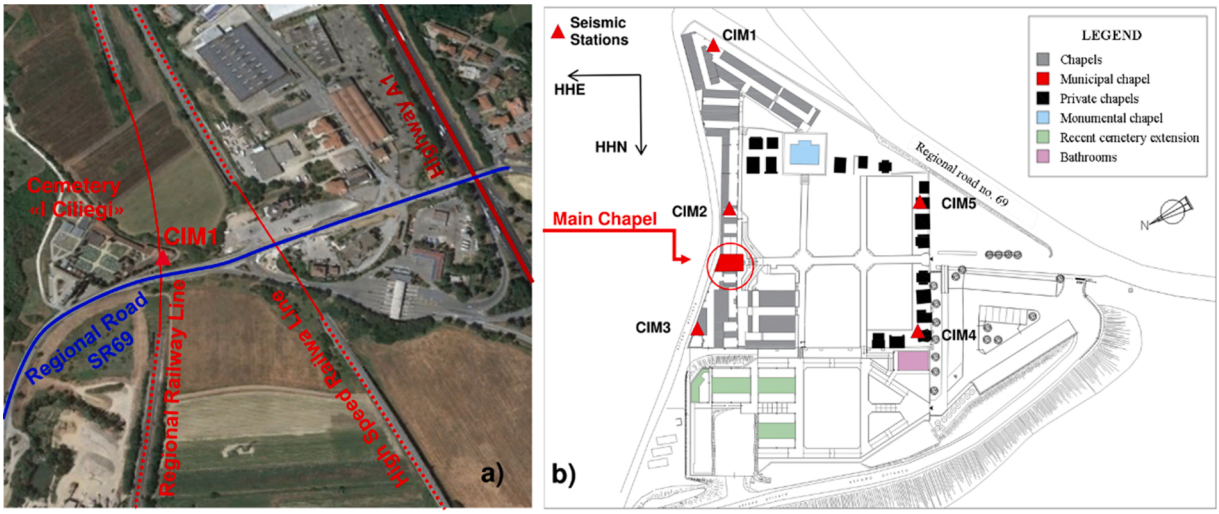

Fig. 1. a) Location of the cemetery in relation to the main sources of vibration. b) Layout of the cemetery with the indication of the monitored points (red triangles).

Under the eastern corner of the monitored area, where CIM1 station was installed, there is a curved railway tunnel of about 400 m in length, which is part of the railway line of regional trains going to and from Florence (Fig. 1a). Approximately 200 m east of the railway tunnel there is the High-Speed railway line with a 200-m long tunnel about 100 m from the closest point of the cemetery (Fig. 1a). About 350 m from the eastern point, there is Highway A1. Next to the cemetery, a few meters below the ground level, there is the regional road SR69, an important transportation link on which many heavy trucks travel.

Blocks of buildings included among the stations CM1, CM2 and CM3 (Fig. 1b), built on the crest of the hill on which the cemetery stands, present significant and very extensive crack patterns. In particular, the main municipal chapel presents vertical and diagonal cracks on the peripheral walls highlighting clear overturning mechanisms of the front and rear façades to the south and north, respectively (Fig. 2a). Such damages are mostly attributable to the slow sliding downstream of the earthy slope behind the chapel, caused by the hydro-geogenic instability of the hill, due to the presence of diverse layers of clay silt soil that have the characteristic of retaining water. Indeed, the rooms that houses the common ossuary and the rear warehouse (Fig. 2d, e), located under the floor of the chapel which shows a continuous crack running along the east-west axis following a zigzag path defined by the joints of the tiles inclined at 45° (Fig. 2b) and is, in turn, inclined both towards the south and north, are often flooded (Fig. 2c). Therefore, the current state of the chapel is very worrisome, because the peripheral walls are detached, and no longer provide the well-known box-like behavior to the construction. On the other hand, it is not possible to exclude a priori that the ground shaking produced by railway and vehicular traffic in the vicinity of the cemetery, may produce an additional damage factor for the built structures, for this reason the seismometric monitoring survey was performed.

2.2. *Estimation of the subsoil properties*

It is widely known that the shaking produced by a seismic event can be subject to the effects of amplification even on a reduced scale due to the mechanical properties of the geological structures present in the first tens of meters from the surface. Regarding Italy, the first observations of the phenomenon date back to the descriptions of the surface effects of some of the strongest seismic events of the last century, when some of the most important geophysicists noticed the different behavior between rigid soils and less compact ones [20,21]. More recently, the study of so-called site effects has appeared more and more important after the devastating earthquakes of Michoacán (19/9/1985, Mexico, M = 7,9) and Loma Pieta (17/10/1989, USA, M = 6,9) [22,23]. The procedure of assessing the mechanical properties of surface geology aimed at evaluating ground shaking due to the propagation of seismic waves, i.e. microzonation, has thus become a useful investigation method for defining the analysis of seismic risk, mostly in urban areas. The objective of the microzonation is to estimate the frequency response of the examined site, in order to quantify the site amplification in terms of amplitude and frequency. One of the most widely known method used to describe the effect of the amplification was developed by Japanese seismologist Akito Nakamura at the end of the 1980s [24], inspired by the work of Nogoshi and Igarashi [25]. Nakamura's technique is a spectral analysis of seismic ambient noise data recorded by a single triaxial seismic station that uses the ratio between the Fourier spectrum of the horizontal and the vertical components to find out the resonance frequency of the site.

Many studies providing a theorical interpretation of this method that have been carried out in recent years were thought to be an empirical technique lacking theorical grounds [26,27]. In the years 2000–2004, the EU-funded SESAME project defined the guidelines for using seismic environmental noise for the definition of ground amplification effects [28]. In recent years, many applications have been carried out and the technique is ordinary practice in the professional activity of microzonation. The Nakamura technique, also known as HVSR (H over V Spectral Ratio), involves the calculation of the average spectral ratio of the horizontal components against

a)

b)

c)

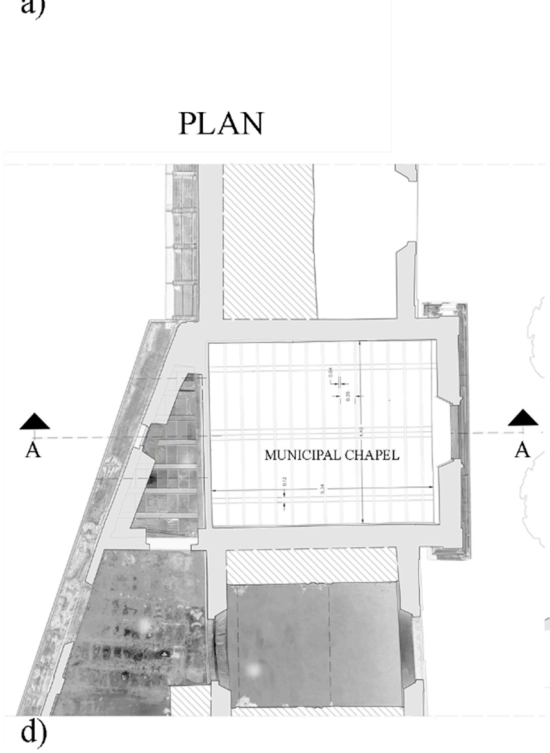

d)

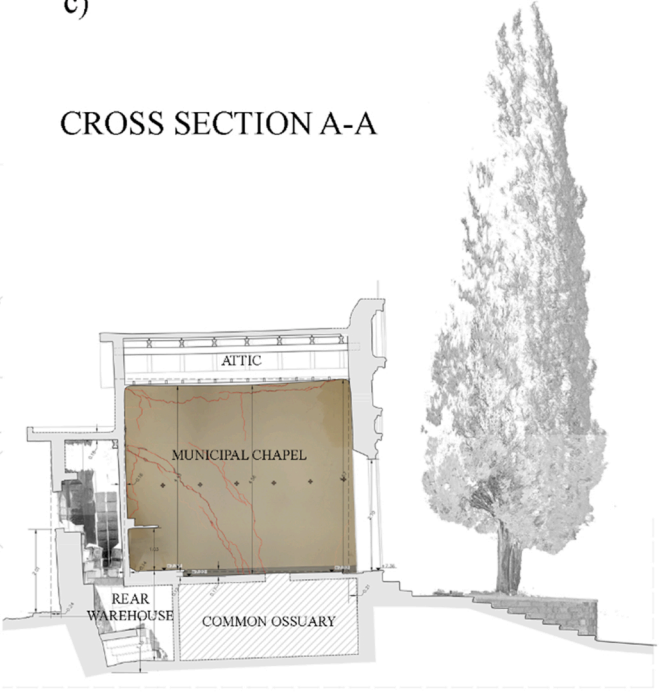

e)

(caption on next page)

Fig. 2. a) Front façade overturning of the main chapel, b) zig-zag crack running along the inside floor of the chapel, c) presence of stagnant water in the rear warehouse, d) plan, e) cross section.

Table 2
Values of subsoil resonance frequency (Fo) in Hz, estimated from HVSR.

Code	N/V [Hz]	E/V [Hz]	H/V [Hz]
CIM1	1.79	1.78	1.79
CIM2	2.07	2.11	2.09
CIM3	2.26	2.29	2.28
CIM4	3.14	3.19	3.16
CIM5	2.79	2.93	2.85

Table 3
Variations in percentage of the thickness of subsoil amplificative layer as obtained applying Eq. (3) to each seismic stations with respect to the CIM1 station, located just above the railway tunnel at the NE corner of the cemetery and which exhibits the lowest value of resonance frequency from HVSR.

Code	Thickness of amplification subsoil [%]
CIM1	H1
CIM2	86% of H1
CIM3	76% of H1
CIM4	57% of H1
CIM5	63% of H1

the vertical ones, in the hypothesis that this one is not affected by amplification and its spectral content is representative of the source and propagation content. Moving from such a hypothesis, we can say that the HVSR, in the presence of a clear acoustic impedance between the amplification layers and the rigid subsoil, highlights the spectral content of the propagation inside the surface geology that produces the amplification effect on the ground, thus making it possible to estimate the resonance frequency of the site.

In the present case study, for each measurement site, spectral ratios were calculated over intervals of 120 s without overlapping (for a more detailed description of the software used please refer to Azzara et al. [29]). All hourly spectral ratios were arranged in order to estimate the representative average spectral ratio for each measurement point. The data analysis and plotting were performed by using the Seismic Analysis Code – SAC [30,31] available at https://ds.iris.edu/ds/nodes/dmc/software/downloads/sac/.

From the reading of the average HVSR ratios and those relating to the single horizontal component for each seismic station, the values of the estimated resonance frequencies are shown in Table 2. The very narrow standard deviation associated with each average ratio seems to confirm the stationarity of the signals. The presence of such clear spectral peaks leads one to hypothesize that for each measurement point it is possible to consider a typical one-dimensional structure characterized by a sharp impedance contrast between the amplification layer and the rigid subsoil. In such a hypothesis, it is possible to use the formula of the quarter of wave (see, for example, [32–34]) to relate the resonance frequency (F_o) to the velocity of shear waves (V_s) and the thickness of amplifying layers (H):

$$F_0 = \frac{V_s}{4H} \tag{1}$$

Taking into consideration the frequency peak values reported in Table 2, it is evident that, even at such a close distance, the seismic stations show resonance frequencies that are highly different from each other. In the reasonable hypothesis that the velocity of shear waves (V_s) is the same in all monitored points, applying Eq. (1) to each measurement point, it will result that for the i-th point the thickness of the resonant layer can be written as:

$$H_i = \frac{V_s}{4F_{0i}} \tag{2}$$

In this way the ratio between the thicknesses in two different measurement points, i and j, is equal to the inverse of the ratio between the corresponding resonance frequencies :

Table 4
Velocity profile extracted from the MASW campaign [35].

Depth [m]	Thickness [m]	Velocity (Vs) [m/s]
1	1	100
5.3	4.3	176
34.3	29	296
40.3	6	736

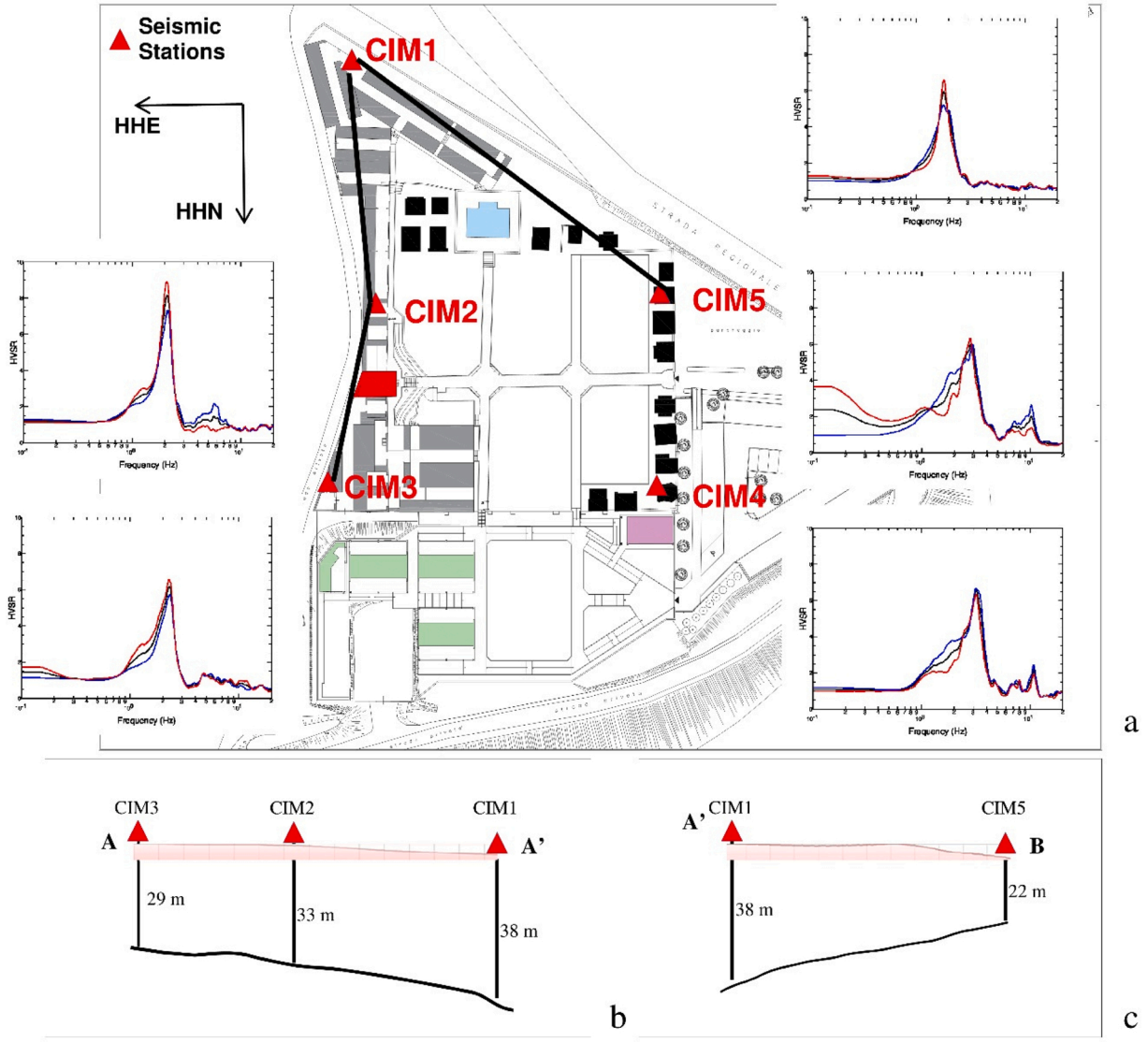

Fig. 3. Interpretation of the results in terms of the topography of the rigid layer beneath the amplifying layer: a) is the cemetery layout, b) and c) are respectively the profiles along AA' and A'B lines shown in a). At the location of each seismic station are also depicted the average HVSR computed over the entire monitoring interval. The black, blue and red curves respectively correspond to EW/Z, NS/Z and H/Z spectral ratio. The frequency axes span between 0.1 and 20 Hz. the amplitude vertical scale is the same for each plot. The frequency corresponding to the spectral peaks for each seismic station are listed in Table 2.

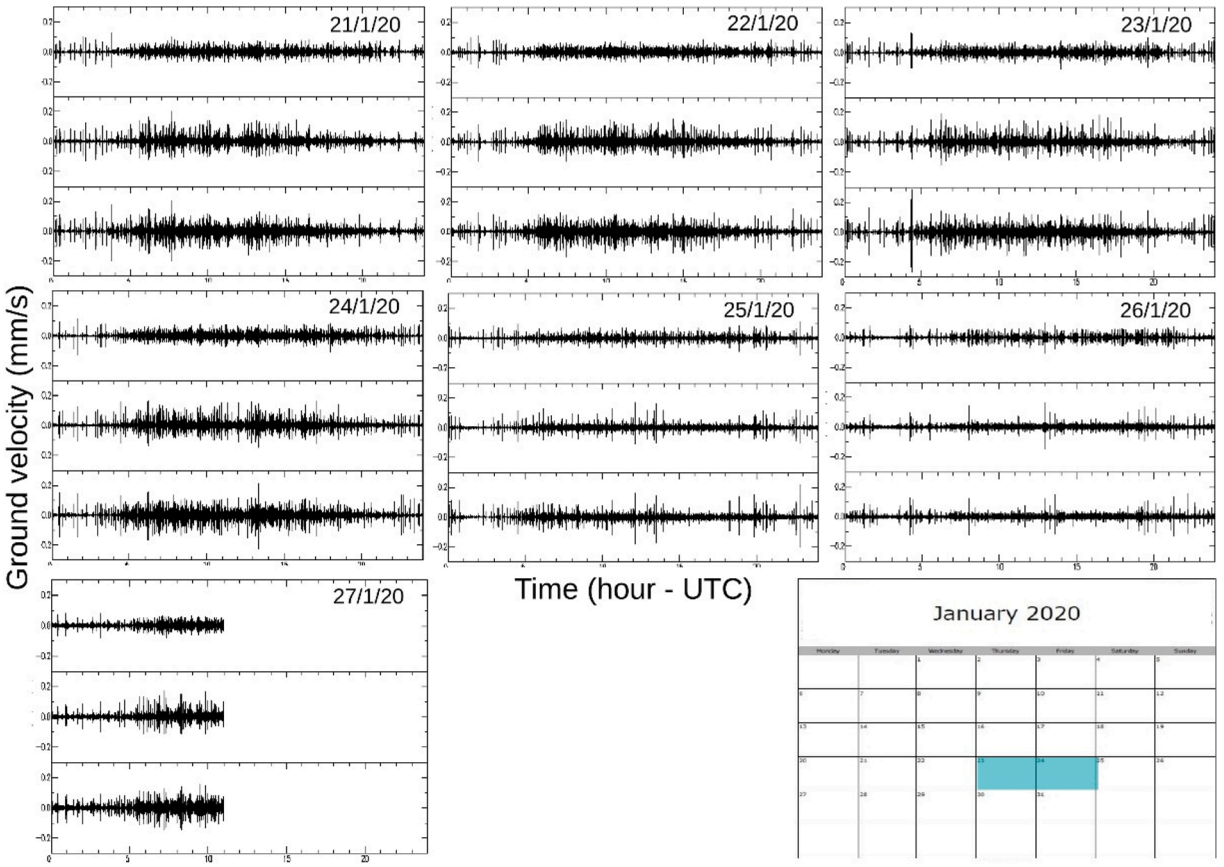

Fig. 4. Daily recordings from CIM1 station. Each graph from to the top down shows respectively the two horizontal components and the vertical one. The time is based on the UTC, one hour behind the local time.

Table 5
Parameter values described by the British BS7385 [17] standard, as reported by UNI 9961 [16].

Class	Type of building	Peak component particle velocity in the frequency band of the dominant pulse		
		4 Hz - 15 Hz	15 Hz - 40 Hz	40 Hz - 250 Hz
1	Frame of reinforced structures. Industrial or commercial buildings	50 mm/s		
2	Non-reinforced structures. Residential buildings or small commercial buildings	exhibits a linear trend from 15 mm/s at 4 Hz to 20 mm/s at 15 Hz	exhibits a linear trend from 20 mm/s at 15 Hz to 50 mm/s at 40 Hz	50 mm/s

$$\frac{H_i}{H_j} = \frac{F_{0j}}{F_{0i}} \tag{3}$$

Given this evidence, it is possible to estimate, in percentage respect one point chosen as reference, how the depth of the rigid interface, which causes the impedance, varies.

Based on the information that can be extracted from the geological report of the cemetery extension [35], the thickness of lacustrine deposits found in this area is 20−25 m high. The area under investigation lies at the westernmost point of the cemetery. The MASW survey conducted during this study provided an estimate of the velocity profile of shear waves (Vs), as reported in Table 4.

According to the information extracted from the geologic report (see [35]) and the results of the HVSR analysis, we can evaluate the geometry of the amplifying layer. Consulting the data in Table 3 it is possible to estimate the slope of the bottom of this layer between the measuring points CIM1 and CIM3. Assuming that the layer thins continuously between these points, we can try to derive an empirical relationship with the intent of evaluating the thickness that should be expected in the area outside the one currently investigated and described by the geological study above mentioned. Following this procedure, it is possible to obtain an equation that allows to estimate the thicknesses of the amplifying subsoil. Computing the coefficients of the linear regression of the distribution of thickness in function of the distance from CIM1 station (Y), it follows that:

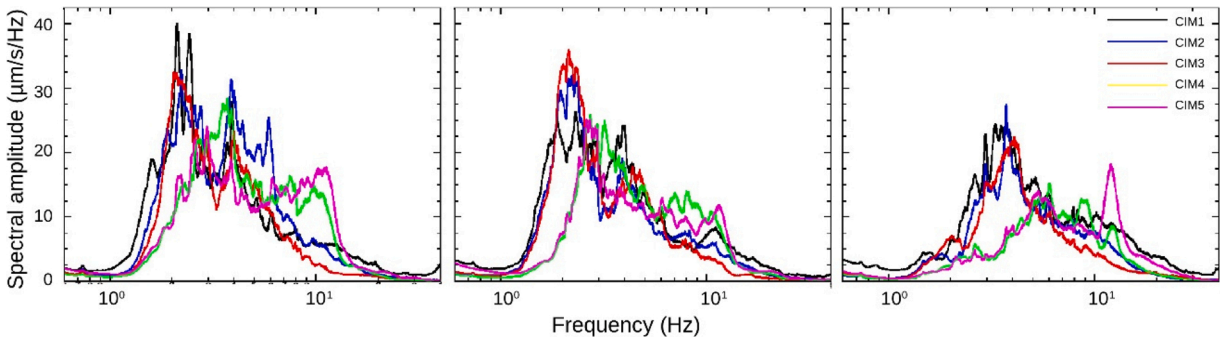

Fig. 5. Average Fourier spectra computed for the entire monitoring period for each measurement point. From left to right, respectively, EW, NS and Z components. The color legend on the left associates the seismic stations to each curve.

$$D = 0.99 - 0.0024Y \tag{4}$$

where D stands for the ratio between the thickness of the amplifying layer in the measuring points CIM2, CIM3 and that of CIM1. Applying Eq. (3), the thickness of the layer at a distance of approximately 140 m from CIM1, which corresponds approximately to the area where the MASW were executed, should be about 66 % of that expected in CIM1. Therefore, according to the results of the geological survey previously conducted, assuming a value of 25 m for the thickness in the area investigated during the survey, we could expect that the amplifying layer in CIM1 should be about 38 m thick.

This value is very close to that obtained by applying Eq. (1), inputting the values: 1.79 Hz for F_0, the resonance frequency of the site, and 275 m/s, the weighted average of the values indicated in Table 4, for Vs:

$$H = \frac{V_s}{4F_0} = \frac{275}{4 \times 1.79} = 38.4m \tag{5}$$

Similar considerations could be made about CIM4 and CIM5 stations, located at the southern edge of the cemetery. At these measuring points, the thickness of the amplification layer should be even smaller.

Fig. 3 shows a geometrical interpretation of the results obtained where two profiles are hypothesized: along the line CIM1-CIM2-CIM3 and the line CIM1-CIM5. It is clear that it might be useful to carry out some other temporary measurements along the perimeter and inside the cemetery to collect further data in order to verify this interpretation.

Another aspect that could be taken into consideration is the width of the HVSR peaks at the different measured points. Despite the fact that ambient noise tends to underestimate the amplification factors, it would seem quite evident that the data recorded by the seismic station installed at the CIM2 point show a spectral peak of the HVSR that is certainly higher than those detected at the other measurement points. This could be a sign that this area is probably the one affected by more pronounced amplification effects as compared to other areas. This area is not far from the currently closed chapel, which has suffered the most significant damage compared to the other buildings inside the cemetery.

3. Analysis of the vibrations

3.1. Estimate of the reference parameters and comparison with the limits set by the regulations

The previously mentioned standard defines the guidelines for the measurement and processing of data. In particular, UNI 9916 [16] identifies velocity as the most suitable physical quantity for measuring vibrations in terms of the effects of damage on buildings, and defines two parameters that provide a quantitative measure of vibrations and set the minimum admissible limits according to the type of source that produces vibrations and to the frequency content:

3.1.1. Peak particle velocity

It is defined as the maximum value in a time interval of the modulus of the velocity vector in a three-dimensional space.

$$p.p.v. = max\left(\sqrt{X^2 + Y^2 + Z^2}\right) \tag{6}$$

3.1.2. Peak component particle velocity

It is the maximum value in a fixed time interval of the modulus of one of the orthogonal components of motion measured simultaneously.

$$p.c.p.v. = max(|C|) \tag{7}$$

where C stands for X, Y, Z orthogonal components.

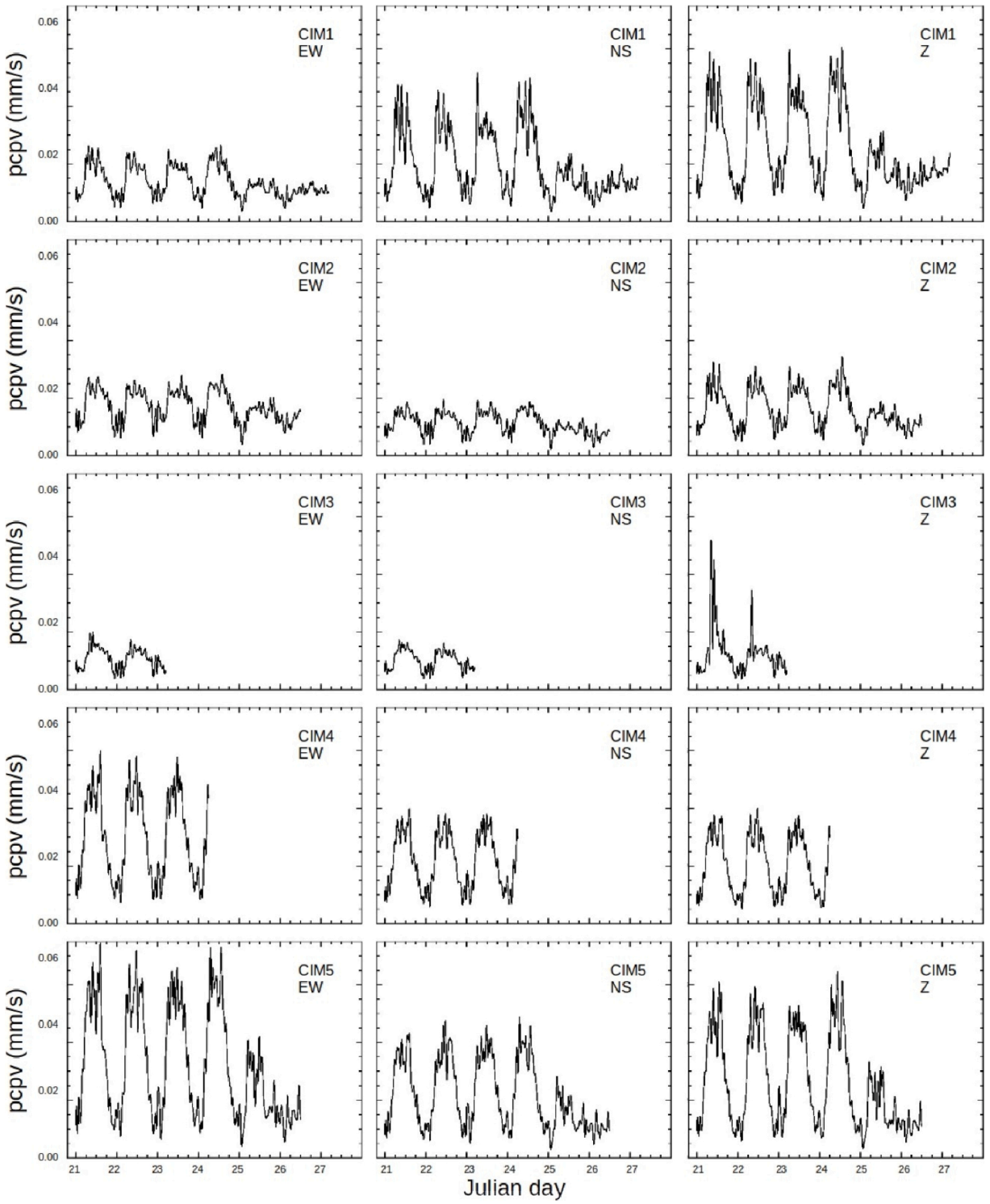

Fig. 6. Time distribution of the peak component particle velocity (p.c.p.v., Eq. (7)), computed for each component of each seismic station, from left to right respectively EW, NS and Z components.

For short-term vibrations, in order to exclude the triggering of fatigue phenomena, the standard provides that the p.c.p.v. should be taken into account. For vibrations caused by explosions, machines and railway or vehicular traffic the correct parameter is the p.p.v.

The standard provides tables of reference values that define the maximum effect of vibrations that are not dangerous for the safety

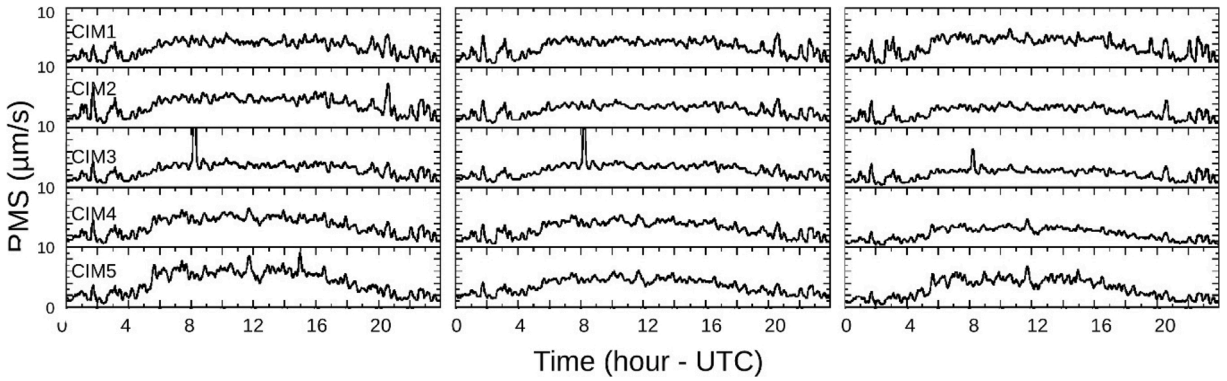

Fig. 7. Displacement waveforms recorded on January 22nd, 2020 by the seismic stations installed inside the cemetery. From left to right HHE, HHN, HHZ components are shown.

Table 6
The maximum displacement between 1-4 Hz recorded on January 22nd, 2020 by the monitoring seismic stations.

Code	HHE [μm]	HHN [μm]	HHZ [μm]
CIM1	3.7	4	5.3
CIM2	5.1	3.6	3.5
CIM3	9.8	5.1	16
CIM4	2.3	3.6	0.7
CIM5	2.1	2.2	1

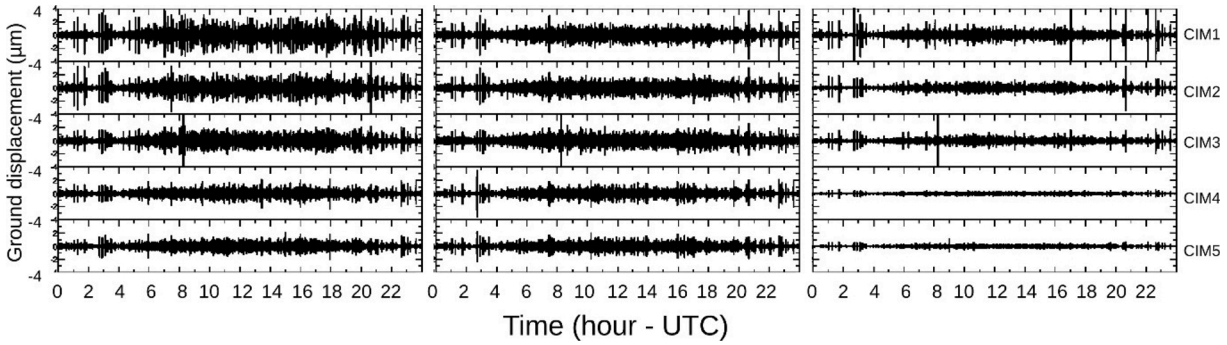

Fig. 8. Daily trend of RMS on January 22nd, 2020 for each seismic station installed inside the cemetery. From left to right respectively EW, NS, Z components are shown.

of buildings. These values are related to the type of sources, the classification of buildings and, for some specific cases, the involved frequency bands.

The position of the monitored area exposes it to the presence of numerous sources of vibrations: two railway lines, the highway, a regional road. As regards to the former, it is pVossible to reconstruct the occurrence of the oscillation sources starting with the information available online from the Italian Railway Company, Trenitalia, timetable.

The information from the online schedule provides a rough indication of the passages along the railway lines. Trains from Rome to Milan and from Rome to Venice in both directions were considered, but it was not possible to obtain any information on the passage of either high-speed trains operated by the company ITALO or freight trains. This notwithstanding, the main passages in both directions are mostly evident on work days from 6 a.m. to 11 p.m. It is likely that, on holidays, the number of passages decreases and occurs on a reduced basis. The same considerations can be made for the other two sources of vibrations, the highway and the regional road, but in both cases, it is not possible to estimate the number of vehicle passages. What has been observed is quite evident in Fig. 4, which shows the daily trends of the signal recorded at the CIM1 station during the entire monitoring period. It is, in fact, possible to notice that during weekends there is a remarkable reduction of both the width and duration of the vibrations in the area.

Indeed, it is very hard to understand to which means of transportation the numerous recognizable peaks in the daily trend of the seismic ambient noise correspond. Vibrations of higher amplitude are distributed throughout the day. During the night or late evening

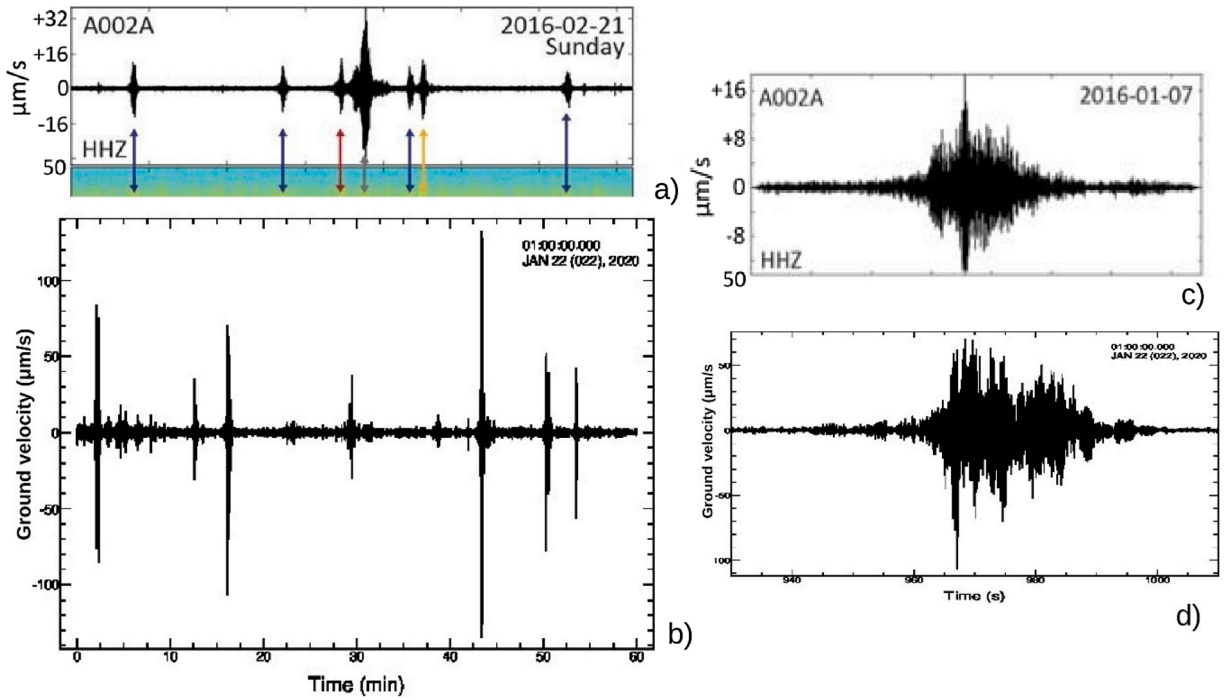

Fig. 9. Qualitative comparison between the signals recorded by seismic stations CIM1, b) and d), and those published by Fuchs et al [12] at train passages a) and c), (modified from [12]).

hours, it is possible to more clearly recognize the presence of sharp peaks due to transients that are recorded by all the seismic stations. This effect is probably due to the fact that during the night the average level of ambient noise decreases significantly as compared to the daytime and, therefore, the transients are more evident.

In this case study, it seems more correct to refer to the British standard, BS7385 [17], that is applicable to buildings less than 3 floors and valid for vibrations generated outside the building and for measurements made at its base, instead of the Swiss standard, SN 640312 [19], which, although specific for road and rail traffic with frequencies above 8 Hz, refers to measurements made in the highest parts of the structures. Table 5 shows the reference values defined by the aforementioned British standard, reported in the Italian standard [16].

The standard aims at comparing the values in Table 5 by UNI 9961 [16] with the p.c.p.v. parameter defined by Eq. (7). If the system were in resonance conditions, the values would be reduced by 50 % and in the case of transients with frequency content lower than 4 Hz, the minimum limit specified in the table, it is required that the displacement does not exceed the value of 0.6 mm, regardless of the frequency.

Before calculating the p.c.p.v. it is necessary to find out the frequency band of the vibrations for the measurement points. The average Fourier spectra (FFT) (Fig. 5) were computed as the geometrical mean of the spectra computed on consecutive windows 120 s in length.

Fig. 5 shows the average velocity spectra calculated for each measurement point and each component of motion. In particular, it is possible to notice that the frequency content of the ground vibration recorded by the seismic stations is, generally, concentrated in the spectral band between 1 and 20 Hz, despite the differences between the different locations. For the stations located in the upper part of the cemetery (CIM1, CIM2, CIM3) the spectral band narrows down to 1–9 Hz, for those in the lower part (CIM4, CIM5) it shifts towards higher frequencies, between 2 and about 20 Hz.

At a low frequency, all the stations and components show the presence of a comparable amplitude peak centered around 0.2 Hz, which can reasonably be attributed to environmental factors.Given the previous considerations, in order to represent the temporal variation of the maximum amplitude of each component of the motion, the p.c.p.v. was computed over the entire monitoring period in the spectral band between 4 and 15 Hz, as required by the aforementioned standards. The maximum of each component on each floating window of 120 s with an overlap of 60 s was estimated. The curves have been smoothed by using the arithmetic smoothing algorithm provided by SAC code. Fig. 6 shows the trends of the p.c.p.v. for each component of the motion for each measurement point over the entire monitoring period.

The distribution of maximum peak values highlights the daily periodicity of ambient seismic noise, which is in line with what was previously observed.

Seismic stations CIM4 and CIM5, located in the lower part of the cemetery area and closer to regional road SR69, show, in the considered frequency band, higher maximum values as compared to the stations installed in the upper part, which are closer to the tunnel of the regional railway line.

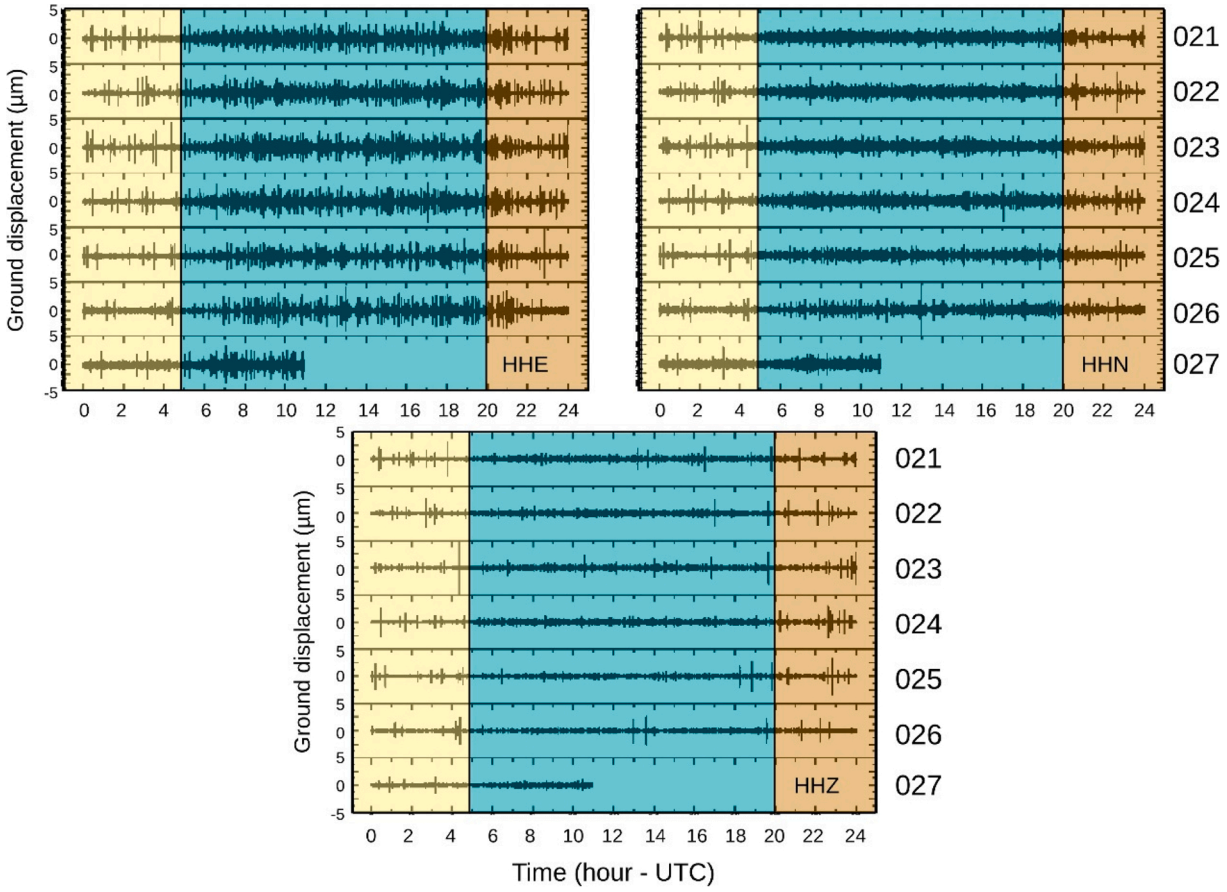

Fig. 10. Displacement waveforms recorded by CIM1 station throughout the monitoring period. The numbers on the right indicate the Julian day corresponding to each recording. The three colored bands identify the three different periods of the day in which similar trends are recognized. The two boxes at the top are related to the horizontal components, EW and NS, respectively from left to right. The box below relates to the vertical component of the motion.

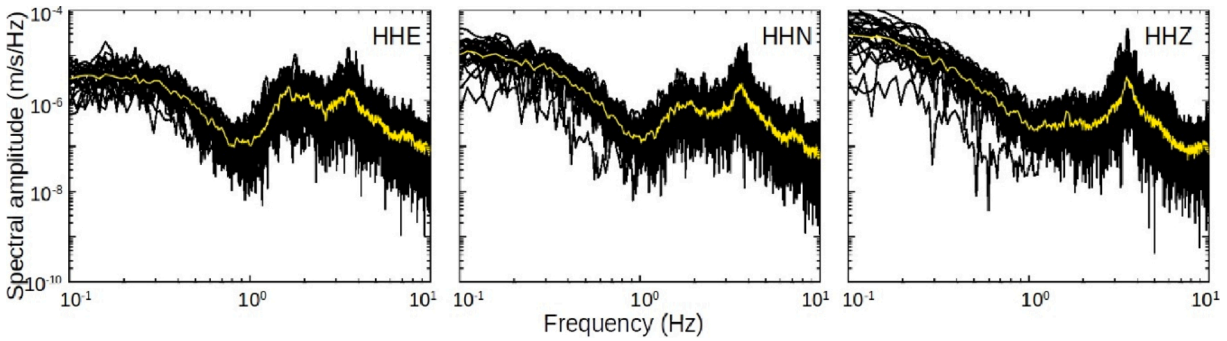

Fig. 11. Distribution of the Fourier spectra of the first class of transients (black curves). The yellow curves are the average spectra computed for each component of motion, from left to right EW, NS and Z.

The maximum values of the p.c.p.v. between 4 and 15 Hz, however, do not exceed 0.25 mm/s, thus placing themselves well below the requirements of the standard (see Table 5).

All the previous considerations are applicable to the frequencies between 4 and 15 Hz, as established by the BS 7385 standard. The average spectra of the signals recorded in the different measurement points, however, show that, especially for the stations located in the upper part of the cemetery area (CIM1, CIM2, CIM3), most of the energy is concentrated in the frequency range of 1−4 Hz.

For frequencies below 4.0 Hz the regulation requires that the displacement does not exceed 0.6 mm regardless of the frequency. The recorded waveforms below 4.0 Hz were then filtered and integrated to obtain the displacement in millimeters. Fig. 7 shows an example

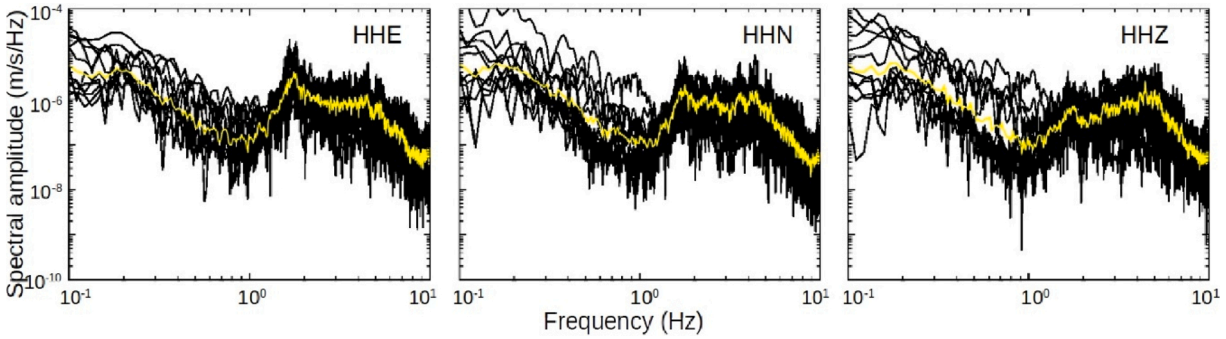

Fig. 12. Distribution of the Fourier spectra of the second class of transients (black curves). The yellow curves are the average spectra computed for each component of motion, from left to right EW, NS and Z.

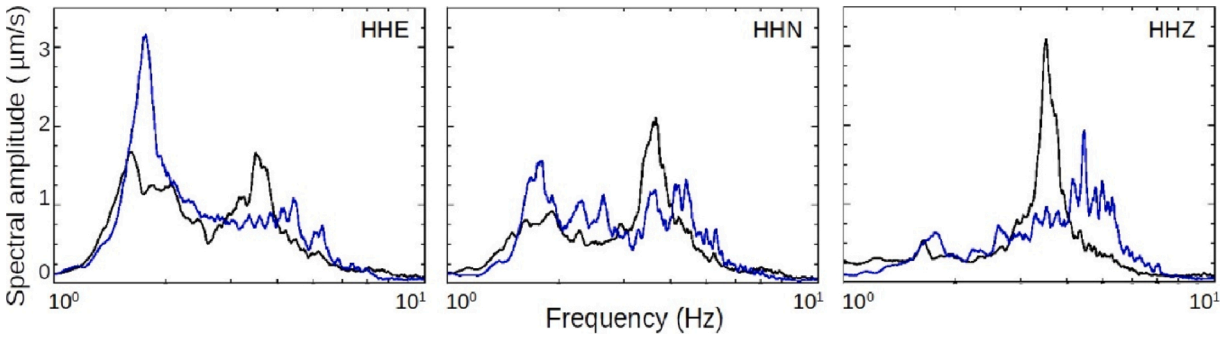

Fig. 13. Comparison between the average Fourier spectra of the first class (black curves) and the second class (blue curves).

of the ground displacement recorded by all seismic stations in the 1−4 Hz band during a work day.

The maximum values recorded by the seismic stations are listed in Table 6. The highest displacements are recorded at the stations located in the upper part, which have values that, on average, are about double when compared to the stations in the lower part, which, in particular on the vertical component, record shaking that slightly exceed one micron. Even taking into account that the absolute maximum value, the one detected in CIM3 and attributable to one of the disturbances mentioned above, is around 0.016 mm, the maximum values of detected displacement are well below that defined by the standard.

3.2. An attempt to classify transients

For the sake of completeness, even if not required by regulations, the trend of the RMS average over the entire recording period was calculated. The RMS calculation was executed on intervals of 120 s overlapped by 60 s. Fig. 8 shows the RMS trends for one of the monitored days.

The RMS trend highlights what was previously observed: the average daily oscillation level begins to increase from early morning, around 6 a.m. (local time) until about 7 p.m. (local time), when it begins to decrease. The transients that stand out from the background noise and show the highest amplitudes are concentrated during the night and in the late evening. The values of the maximum and average amplitudes, as already observed, remain at considerably lower levels than those which, according to the regulations, can cause damage to the building structures.

The task of discriminating which of the multiple transients recorded daily by the seismic stations are attributable to the passage of trains and which are due to other causes is not easy to perform.

A substantial support, at least qualitative, can be provided by a comparison with the signals recorded in the presence of railway traffic, as available in literature. In particular, Fuchs et al. [12] reports numerous examples of seismometric recordings of train passages. Fig. 9 shows the comparison between the signals recorded by CIM1 station (the one placed just above the railway tunnel) and the ones published in Fuchs et al. [12].

The signals shown in Fig. 9 are among the most energetic recorded by the CIM1 station, their maximum values of amplitude reaching some hundreds of microns, well below the limits set by the current regulations.

In order to classify the different types of signals recorded by the seismic stations, we first tried to recognize, in the daily records, the intervals in which similarities of behavior were found and, subsequently, by analyzing the individual transients, we tried to identify the signals showing spectral response analogies.

Fig. 10 shows the displacement waveforms recorded by the CIM1 station throughout the monitoring period. Observing the daily

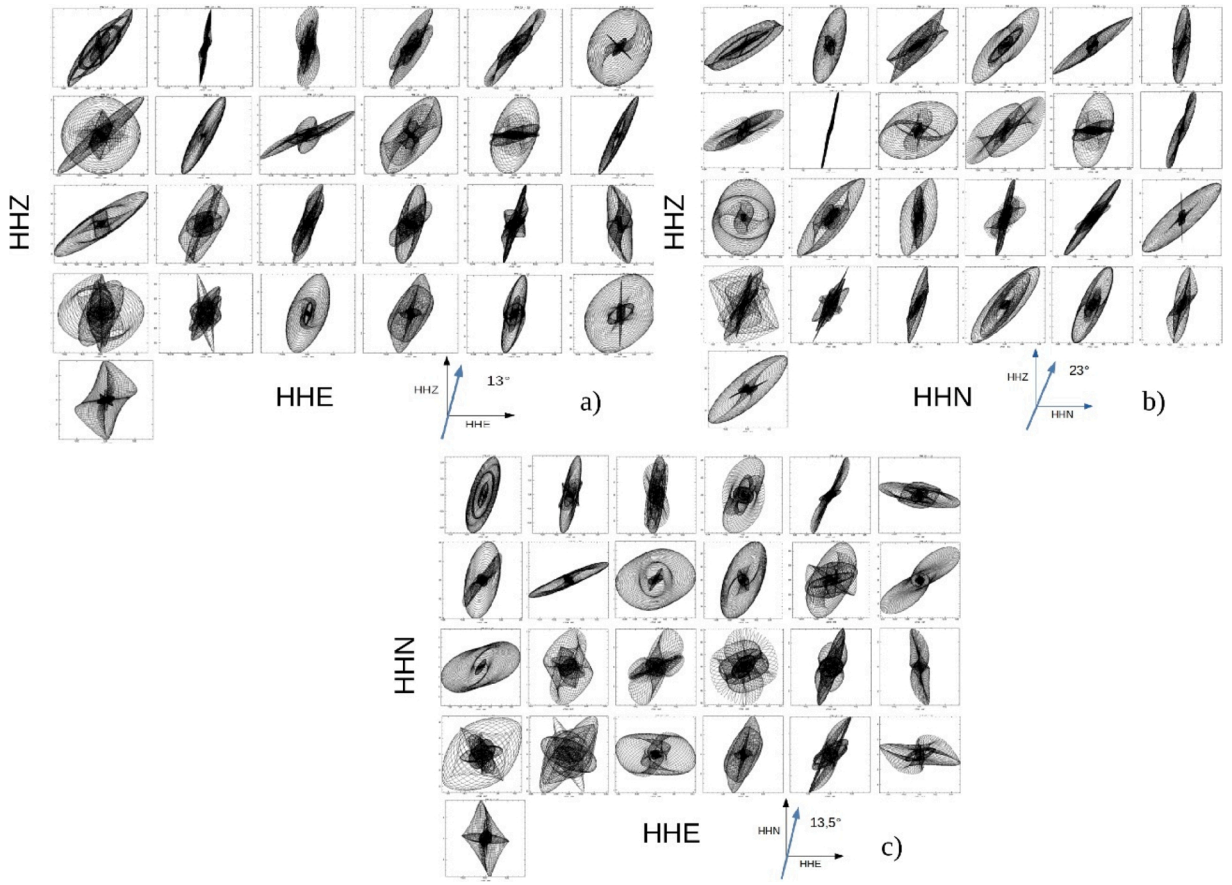

Fig. 14. Particle motion of ground displacement in the coordinated planes in the presence of transients: a) NS-Z, b) EW-Z, c) EW-NS. The blue arrows indicate the average direction of shaking in the planes considered.

records it seems reasonable to identify three periods throughout the day that show similar trends: the night period, between midnight and 5 a.m. (UTC), the central period of the day (from 5 a.m. to 8 p.m.), and late evening (from 8 p.m. to midnight).

Every single transient was analyzed in the frequency domain, in order to identify those exhibiting similar spectral behavior. The Fourier spectra were calculated for each selected signal. The selection was made on all the recordings from CIM1 station, focusing on the first of the selected periods, at night, in which the presence of the transients is highly evident. By comparing the spectra, two classes were found, which include approximately 52 % of the analyzed signals. Figs. 11 and 12 show the spectra of the selected signals and the spectral average for each class.

The first class exhibits a main spectral peak centered on 3.5 Hz. It generally occurs with maximum amplitude on the NS and Z components and minimum amplitude on the HHEW direction.

The second class is characterized by the presence of a main peak around 1.7 Hz, which is more evident on the EW component; most of the spectral content is distributed approximately in the frequency band between 1.5 and 5 Hz. Above this value, the spectra decrease constantly. Fig. 13 presents the comparison between the spectra of the two classes.

In order to identify the area of origin of the sources of the recorded signals, an attempt was made to evaluate the vector compositions of the motion in the three coordinated planes, i.e. HHE-HHN, HHE-HHZ, HHN-HHZEW-NS, EW-Z and EW-NS respectively.

This procedure allows one to identify the predominant directions of origin of the wave front. In Fig. 14 the particle motion related to the signals that have a dominant spectral peak around 3.5 Hz are shown. The waveforms were filtered in a very narrow band around the predominant frequency and integrated to obtain the ground displacement. Once the angles of orientation of the particle motion in the different planes were measured, the average directions of the movement in each coordinate plane were calculated (blue arrows in Fig. 15).

From Fig. 15 it is possible to observe that the direction of ground shaking associated with each single transient shows a large variability. The average direction of ground motion along the HHE-HHZ and HHN-HHZ planes indicates shaking predominantly in the vertical direction. On the horizontal plane, an average direction of shaking is identified along an axis at about 13° with respect to the HHN axis. Unfortunately, the results obtained are not sufficient to clearly identify the area producing the recorded signal.

Further considerations can be made for the CIM3 station, which exhibits transient episodic values that show peak values above the maximums recorded in the other stations, in particular on the vertical component (Fig. 16). These transients are recorded only in the

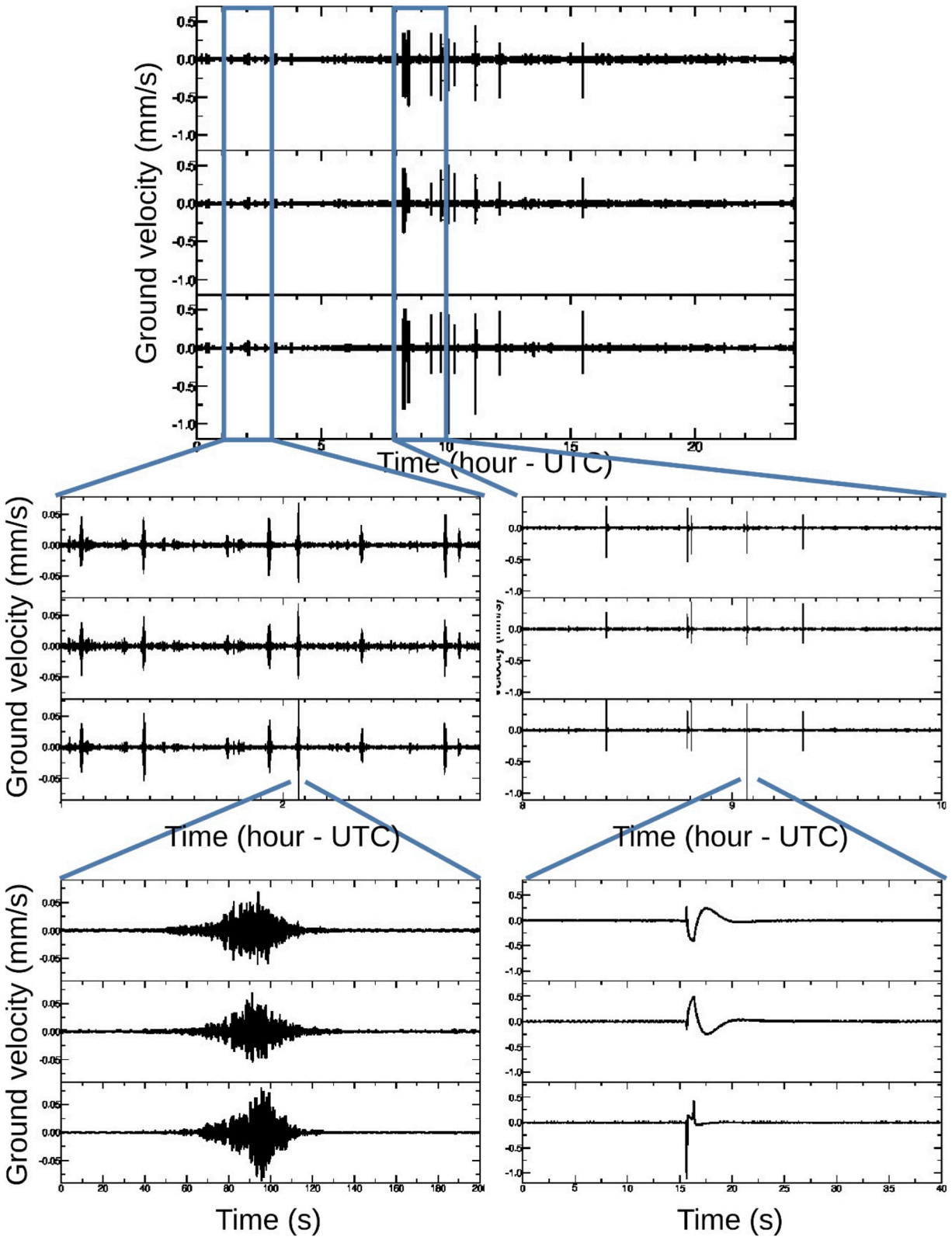

(caption on next page)

Fig. 15. a) Time series recorded on 21 January 2020 at the CIM3 site, from top to bottom respectively EW, NS, Z component. b) and c) magnification of the signals recorded during two hours of night (02:00 a.m. - 04:00 a.m. local) (b) and daytime (09:00 a.m. - 11:00 a.m. local) (c); d) enlargement of one of the signals due to a vehicle or train passage near the cemetery; e) enlargement of one of the disturbances detected during working hours by the seismic station CIM3.

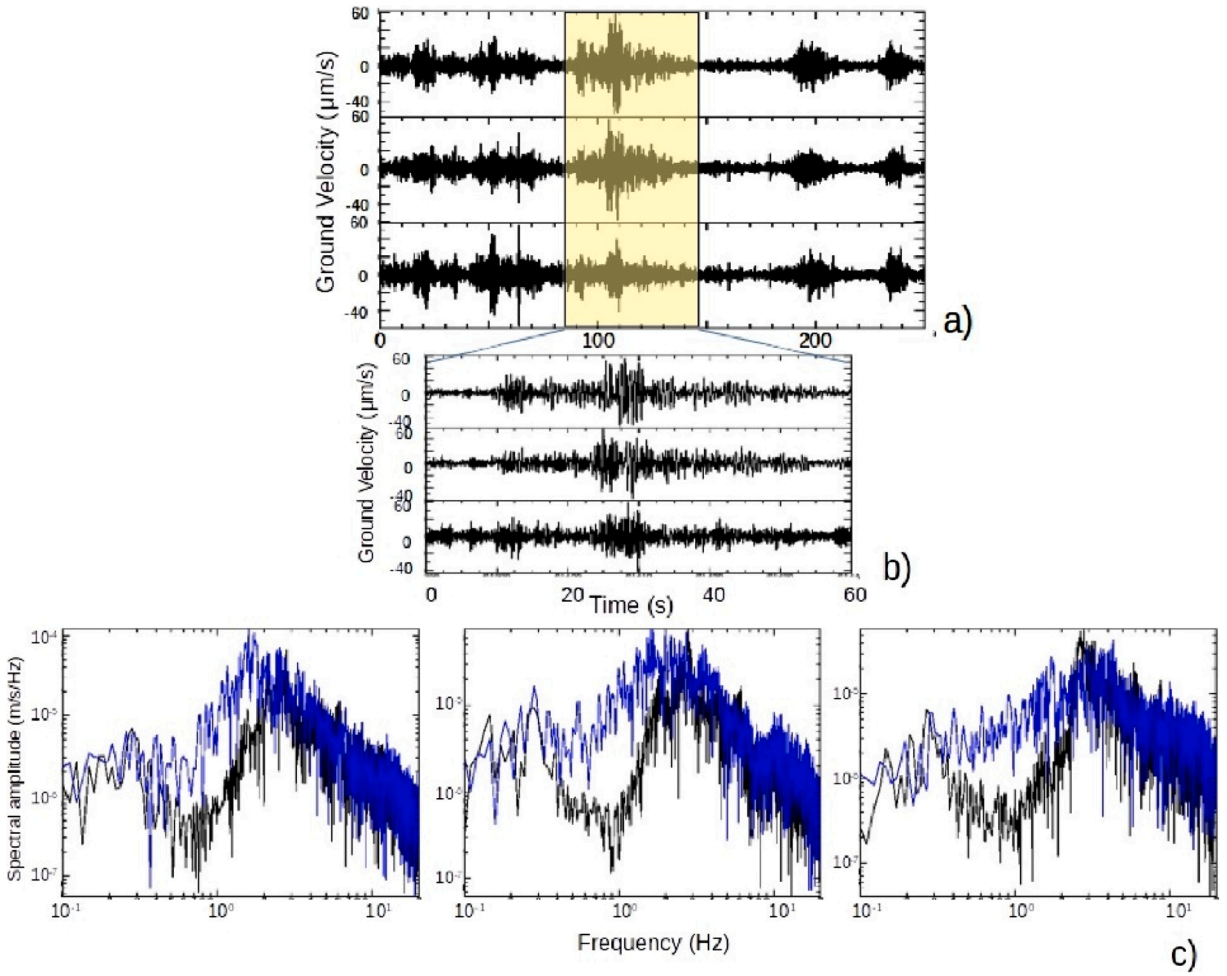

Fig. 16. a) Waveforms recorded by the seismic station CIM1 along the three components of the motion, containing the seismogram of the earthquake of 24th January 2020 at 17:02 (UTC), from top to bottom EW, NS, Z components; b) Seismogram of the earthquake. c) Spectral comparison between the FFT of the seismogram (blue curves) and that calculated in an interval containing only transients (black curves), EW, NS, Z from left to right respectively.

Table 7
List of seismic events that occurred during the monitoring period and recognizable in the recordings of the installed seismic stations (from INGV, [36]).

Time [UTC]	Latitude	Longitude	Depth [km]	Magnitude (Mw)	Event Location Name
2020-01-21T18:51:14.310	44.0077	10.6683	53.1	2.4	6 km E Bagni di Lucca (LU)
2020-01-21T19:04:33.980	44.1188	10.7393	11.2	3	2 km NW Cutigliano (PT)
2020-01-24T17:02:48.240	44.4513	12.3578	4.6	3.4	Costa Ravennate (RA)
2020-01-24T17:55:15.242	38.2553	39.2001	10	6.6	Turkey
2020-01-24T23:41:03.640	44.3163	12.1693	20.6	2.9	12 km S Ravenna (RA)
2020-01-26T06:31:58.826	51.2086	−17.9879	19.5	6.1	Andreanof/Aleutian Islands
2020-01-26T16:26:03.250	43.9055	12.6112	25.6	3	2 km N Montefiore Conca (RN)

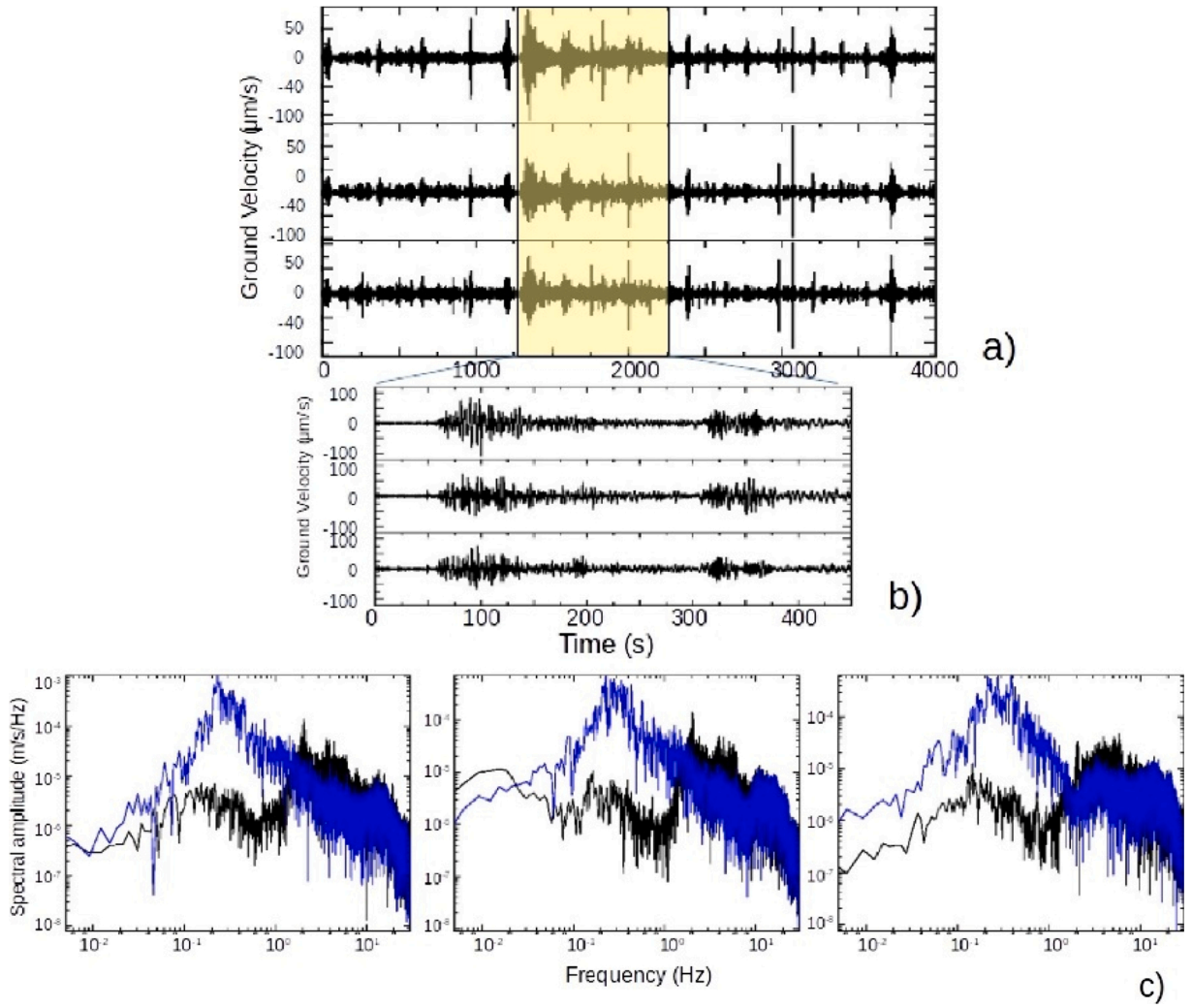

Fig. 17. a) Waveforms recorded by the seismic station CIM1 along the three components of the motion (from the top to bottom: EW, NS, Z), containing the seismogram of the earthquake occurred in Turkey on January 24th, 2020 at 17:55 (UTC). b) Seismograms of the earthquake. c) Spectral comparison between the FFT of the seismogram (blue curves) and that calculated in an interval containing only the transients (black curves), EW, NS, Z from left to right respectively.

central period of the day (Fig. 16e), which is characterized by full working activity. They have a completely different waveform from those that can be associated with train passages (Fig. 16d). The total absence of disturbances of the same type during the non-working period of the day and the fact that the seismic station was installed inside the room where maintenance materials and tools are stored, reasonably suggests that the transients are attributable to the presence of service personnel.

3.3. Analysis of the seismograms

During the monitoring period some seismic events occurred on the national territory and outside, reported in the INGV National Seismic Network Database. Table 7 lists the events clearly recognizable in the records of the seismic stations installed.

The most energetic local event recorded during the monitoring period occurred off the Ravenna coast on January 24th, 2020 at 17:02 (UTC), at more than 100 km from the investigated area. The seismograms of this event were compared with the waveforms of transients recorded by the seismic monitoring stations in order to compare the amplitudes of the observed seismic shaking with that produced by vehicular or railway traffic.

Fig. 16 shows the comparison between the transients and the seismogram of the earthquake off the coast of Ravenna recorded by the seismic station CIM1. It is possible to observe that the width of the motion produced by the transients can be compared to that produced by the earthquake which occurred 115 km from the seismic station, taking into account that in the case of the seismograms the bulk of the spectral content is distributed in the 0.3–3 Hz frequency band.

A similar situation can be observed for the earthquake, Mw 6.6, occurred in Turkey on January 24th, 2020 at 17:02 (UTC),

approximately 2400 km from the area under study.

Fig. 17 shows the comparison in the time and frequency domain between the signals recorded by the CIM1 station in the presence of transients and following the earthquake in Turkey. Also in this case it is possible to note that the amplitude of the ground motion recorded during the transients is of the same order as the seismogram recorded during the earthquake, taking into account that, in this case, the frequency content of the seismogram is concentrated in the 0.6−2 Hz band where the spectral amplitude of the seismic ambient noise recorded in the cemetery area is very small compared to what is found at high frequency.

4. Final considerations

The analysis of the signals recorded during the monitoring period has made it possible to define the spectral properties of the subsoil within the study area. From the HVNSR analysis (Nakamura's technique), the fundamental frequency of soil is distributed between 1.7 and 3.2 Hz, according to the position of the seismic station. The values obtained from the analysis of the signals are in good agreement with those indicated by the geological analysis carried out in 2016. Referring to the velocity profile of the seismic waves reported in the aforementioned geological report, it was also possible to estimate the thickness of the amplifying layer, in the hypothesis of a clear acoustic impedance contrast between this and the underlying geological layer.

With reference to the regulations in force, the amplitudes of movement were assessed in terms of displacement and speed of the shaking associated with the presence of transients attributable to vehicular or railway traffic and, in general, to the anthropic activities that take place in the area surrounding the cemetery. The result of the application of the algorithms required by current regulations has produced an estimate of the values of the peak component particle velocity (p.c.p.v.) in the frequency band between 4 and 15 Hz and the maximum displacement below 4 Hz. In both cases, the results obtained are well below the limits set by the regulations. In the absence of a detailed list of train passages on the regional and high-speed lines, it was not possible to clearly associate each single transient with railway passages. A specific analysis was, therefore, carried out on the individual transients recorded by the seismic stations (in particular by the CIM1 station, i.e. the one located above the railway tunnel of the regional line, the closest in a straight line to the High Speed tunnel and to the Regional Road located near the cemetery).

The analysis has permitted to recognize the presence of at least two classes of signals, characterized by a homogeneous spectral behavior. Starting from the spectra of the individual transients, the representative average spectra of the two classes of signals were estimated, which can be considered as reference inputs for a possible execution of numerical modelling modeling of the response of the buildings present in the cemetery area. Finally, the ground shaking produced by the transients was compared to that produced by the earthquakes in the area of the cemetery during the monitoring.

The amplitude of the ground motion produced by transients, associated with vehicular and railway traffic and anthropic activity, was of the order of that recorded on the two most energetic earthquakes also because they have most of the frequency content in bands that extend below the one that is characteristic of the site in the absence of seismic signals. Furthermore, considering that these two earthquakes are either of low magnitude, about 100 km away from the area under study, or of considerable magnitude but located approximately 2400 km away, the observation confirms that the signals produced by daily human activity are indeed of low entity.

Further considerations can be made, in spectral terms, taking into account the building typology of the area under study. This exhibits small single-story buildings, for which it seems reasonable to expect a main frequency of oscillation between 8 and 10 Hz. This such as to exclude the possibility of resonance phenomena both as respect to the frequency content of the signals that produce the main oscillations of the ground, and as respect to the resonance frequency of the ground, estimated by HVSR, which is sufficiently different from that hypothesized for buildings.

All these consideration leads to conclude that in this study case the vibration produced by railway or road traffic cannot produce ground shaking able to determine the observed damages on the building structures. The amplitudes of the transients associated to the traffic are, in fact, under the threshold fixed by the national and international regulation and their spectral band is in a range that leads us to exclude the possibility of double resonance effect. As hypothesized in the text it is more plausible that the damage to the cemetery structures is produced by slow movements associated with the instability of the slope due to retain of water rather than with the vibrations induced by the railway or the road.

Declaration of Competing Interest

The authors declare that they have no known competing financial interests or personal relationships that could have appeared to influence the work reported in this paper.

Acknowledgments

The study was partially funded by the Municipality of Figline-Incisa Valdarno.

Caterina Perugini edited the English version during her internship for the degree course in Languages for International and Business Communication at the University of Siena.

References

[1] N.R. Nakata, R. Snieder, T. Tsuji, K. Larner, T. Matsuoka, Shear wave imaging from traffic noise using seismic interferometry by cross-coherence, Geophysics 76 (6) (2011) SA97–SA106, https://doi.org/10.1190/GEO2010-0188.1.

[2] D.A. Quiros, L.D. Brown, D. Kim, Seismic interferometry of railroad induced ground motion: body and surface wave imaging, Geophys. J. Int. 205 (1) (2016) 301–313, https://doi.org/10.1093/gji/ggw033.

[3] G. Kouroussis, H.P. Mouzakis, K.E. Vogiatzis, Structural impact response for assessing railway vibration inducedon buildings, Mech. Ind. 18 (803) (2017), https://doi.org/10.1051/meca/2017043 (2017).

[4] P. Basekar, D. Vaghela, M. Katakiya, Impact of traffic vibration on heritage structures, Int. J. Adv. Technol. Eng. Sci. 03 (03) (2015). March 2015.

[5] P. Ellis, Effects of traffic vibration on historic buildings, Sci. Total Environ. 59 (1987) (1987) 37–45.

[6] A. Jakubczyk-Galczynska, R. Jankowski, in: Proceeding of The 9th International Conference "ENVIRONMENTAL ENGINEERING", 22–23 May 2014, Vilnius, Lithuania, SELECTED PAPERS, 2014.

[7] G. Bongiovanni, P. Clemente, D. Rinaldis, F. Saitta, Traffic-induced vibrations in historical buildings, in: Roeck De, G. Degrande, G. Lombaert, G. Müller (Eds.), Proceedings of the 8th International Conference on Structural Dynamics, EURODYN 2011, Leuven, Belgium, 4-6 July 2011G, 2011. ISBN 978-90-760-1931-1934.

[8] P. Galvín, J. Domínguez, Experimental and numerical analyses of vibrations induced by high-speed trains on the Córdoba–Málaga line, Soil Dyn. Earthq. Eng. 29 (4) (2009) 641–657, https://doi.org/10.1016/j.soildyn.2008.07.001, 2009.

[9] C. Zou, Y. Wang, J.A. Moore, M. Sanayei, Train-induced field vibration measurements of ground and over-track buildings, Sci. Total Environ. 575 (2017) 1339–1351, https://doi.org/10.1016/j.scitotenv.2016.09.216, 2017 January, Epub 2016 Oct 1.

[10] N. Correia dos Santos, A. Colaço, P. Alves Costa, R. Calçada, Experimental analysis of track-ground vibrations on a stretch of the Portuguese railway network, Soil Dyn. Earthq. Eng. 90 (2016) 358–380, https://doi.org/10.1016/j.soildyn.2016.09.003.

[11] A. Colaço, P.A. Costa, A. Castanheira-Pinto, P. Amado-Mendes, R. Calçada, Experimental validation of a simplified soil-structure interaction approach for the prediction of vibrations in buildings due to railway traffic, Soil Dyn. Earthq. Eng. 141 (February) (2021), https://doi.org/10.1016/j.soildyn.2020.106499, 2021.

[12] F. Fuchs, G. Bokelmann, W.G. AplArrai, Equidistant spectral lines in train vibration, Seismol. Res. Lett. 89 (1) (2018) 56–66, https://doi.org/10.1785/0220170092.

[13] Q. Chen, L. Li, G. Li, L. Chen, W. Peng, Y. Tang, Y. Chen, F. Wang, Seismic features of vibration induced by train, Acta Seismol. Sin. 17 (6) (2004) 715–724, https://doi.org/10.1007/s11589-004-0011-7.

[14] A. Ditzel, G.C. Herman, G.G. Drijkoningen, Seismograms of moving trains: comparison of theory and measurements, J. Sound Vib. 248 (4) (2001) 635–652, https://doi.org/10.1006/jsvi.2001.3807.

[15] G. Bongiovanni, G. Buffarini, P. Clemente, D. Rinaldis, F. Saitta, Dynamic characteristics of the Amphitheatrum Flavium northern wall from traffic-induced vibrations, Ann. Geophys. 60 (4) (2017) S0439, https://doi.org/10.4401/ag-7178.

[16] UNI 9916, Norma Tecnica: Criteri di misura e valutazione degli effetti delle vibrazioni sugli edifici, 1/4/2004 (in Italian), 2014.

[17] BS 7385-2, Evaluation and Measurement for Vibration in Buildings. Guide to Damage Levels from Groundborne Vibration, 1993.

[18] DIN 4150-4153, Erschütterungen im Bauwesen - Teil 3: Einwirkungen auf bauliche Anlagen, 2016.

[19] SN 640312 a, Effet des ébranlements sur les constructions, 2013.

[20] E. Oddone, Gli elementi fisici del grande terremoto Marsicano-Fucense del 13 Gennaio 1915, le osservazioni macrosismiche, Società Tipografica Modenese, Modena, 1915 (in Italian).

[21] F. Esu, B. D'Elia, L'influenza della natura dei terreni sugli effetti del terremoto del 13 Gennaio 1915 nei centri abitati del Lazio Meridionale, Rivista Italiana di Geotecnica, 1966, pp. 299–311, 4bis.

[22] K. Singh, E. Mena, R. Castro, Some aspects of source characteristics of the 19 September 1985 Michoacan earthquake and ground motion amplification in and near Mexico City from strong motion data, Bull. Seismol. Soc. Am. 78 (2) (1988) 451–477.

[23] E. Cramwick, K. King, D. Carver, D. Worley, R. William, P. Spudic, R. Banfill, Site response across downtown Santa Cruz, California, Geophys. Res. Lett. 17 (10) (1990) 1703–1790, https://doi.org/10.1029/GL017i010p01793.

[24] Y. Nakamura, A method for dynamic characteristics estimation of subsurface using microtremor on the ground surface, Q. Rep. RTRI 30 (1) (1989) 25–33.

[25] M. Nogoshi, T. Igarashi, On the amplitude characteristics of microtremor -part 2, J. Seism. Soc. Jpn. 24 (1971) 26–40 (in Japanese with English abstract).

[26] P.-Y. Bard, Microtremor measurements: a tool for site effect estimation? in: K. Irikura, K. Kudo, H. Okada, T. Sasatani (Eds.), The Effects of Surface Geology on Seismic Motion Balkema, Rotterdam, 1999, pp. 1251–1279.

[27] S. Bonnefoy-Claudet, F. Cotton, P.-Y. Bard, The nature of noise wavefield and its applications for site effects studies. A literature review, Earth-Sci. Rev. 79 (3–4) (2006) 205–227, https://doi.org/10.1016/j.earscirev.2006.07.

[28] P.-Y. Bard, C. Acerra, G. Alguacil, A. Anastasiadis, K. Atakan, R. Azzara, R. Basili, E. Bertrand, B. Bettig, F. Blarel, S. Bonnefoy-Claudet, P. Bordoni, A. Borges, M. Bøttger-Sørensen, L. Bourjot, F. Cara, A. Caserta, J.-L. Chatelain, C. Cornou, F. Cotton, G. Cultrera, R. Daminelli, P. Dimitriu, F. Dunand, A.-M. Duval, D. Fäh, L. Fojtikova, R. de Franco, G. di Giulio, M. Grandison, P. Guéguen, B. Guillier, E. Haghshenas, J. Havskov, D. Jongmans, F. Kind, J. Kirsch, A. Koehler, M. Koller, J. Kristek, M. Kristekova, C. Lacave, M. La Rocca, A. Marcellini, R. Maresca, B. Margaris, P. Moczo, B. Moreno, A. Morrone, M. Ohrnberger, J.A. Ojeda, I. Oprsal, M. Pagani, A. Panou, C. Paz, E. Querendez, S. Rao, J. Rey, G. Richter, J. Rippberger, P. Roquette, D. Roten, A. Rovelli, G. Saccoroti, A. Savvaidis, F. Scherbaum, E. Schisselé, E. Spühler-Lanz, A. Tento, P. Teves-Costa, N. Theodulidis, E. Tvedt, T. Utheim, J.-F. Vassiliadès, S. Vidal, G. Viegas, D. Vollmer, M. Wathelet, J. Woessner, K. Wolff, S. Zacharapoulos, Guidelines for the implementation of the H/V spectral ratio technique on ambient vibrations - Measurements, processing and interpretation. Deliverable D23.12 of the SESAME project, Bull. Earthq. Eng. 6 (4) (2005) 1–62.

[29] R.M. Azzara, F. Cara, G. Cultrera, G. Di Giulio, Manuale d'uso dei programmi per lo scaricamento e l'analisi automatica dei dati registrati da un array sismico per lo studio degli effetti di sito, Rapporti Tecnici INGV 25 (2004) (in Italian).

[30] P. Goldstein, D. Dodge, M. Firpo, Lee Minner, SAC2000: Signal processing and analysis tools for seismologists and engineers, in: W.H.K. Lee, H. Kanamori, P. C. Jennings, C. Kisslinger (Eds.), Invited Contribution to' The IASPEI International Handbook of Earthquake and Engineering Seismology', Academic Press, London, 2003.

[31] P. Goldstein, A. Snoke, SAC Availability for the IRIS Community, Incorporated Institutions for Seismology Data Management Center Electronic Newsletter, 2005.

[32] S.L. Kramer, Geotechnical Earthquake Engineering, University of Washington: Prentice Hall International Series in Civil Engineering Mechanics, 1966.

[33] F. Mulargia, S. Castellaro, P.L. Rossi, Effetti di sito e Vs30: una risposta alla normativa antisismica, Il Geologo dell'Emilia-Romagna 25 (2007) 25–38 (in Italian).

[34] S. Parolai, Investigation of site response in urban areas by using earthquake data and seismic noise, in: P. Bormann (Ed.), New Manual of Seismological Observatory Practice 2 (NMSOP-2), Deutsches GeoForschungsZentrum GFZ, Potsdam, 2012, pp. 1–38, https://doi.org/10.2312/GFZ.NMSOP-2_ch14.

[35] P. Innocenti, Relazione geologica per la realizzazione di una nuova struttura loculi e ossarietti e manutenzione straordinaria dei vialetti del cimitero di Incisa, 2016 (in Italian).

[36] M. Locati, R. Camassi, A. Rovida, E. Ercolani, F. Bernardini, V. Castelli, C.H. Caracciolo, A. Tertulliani, A. Rossi, R. Azzaro, S. D'Amico, S. Conte, E. Rocchetti, A. Antonucci, Database Macrosismico Italiano (DBMI15), versione 2.0, Istituto Nazionale di Geofisica e Vulcanologia (INGV), 2019, https://doi.org/10.13127/DBMI/DBMI15.2 (in Italian).